MOL manuscript# 27748

Neurotoxicity of domoic acid in cerebellar granule neurons in a genetic model of glutathione deficiency

G. Giordano, C.C. White, L.A. McConnachie, C. Fernandez, T.J. Kavanagh and L.G. Costa

Department of Environmental and Occupational Health Sciences, University of Washington, Seattle, WA, USA. GG, CCW, LAM, CF, TJK, LGC
 Department of Human Anatomy, Pharmacology and Forensic Medicine, University of Parma Medical School, Italy. LGC

1

Running Title: "Glutathione modulates domoic acid toxicity"

Correspondence: Dr. Lucio G. Costa
                     Department of Environmental and Occupational Health Sciences
                     University of Washington
                     4225 Roosevelt Way NE, Suite 100
                     Seattle, WA 98105
                     Tel (206) 543-2831
                     Fax (206) 685-4696
                     Email: lgcosta@u.washington.edu

Number of text pages:	41
Number of tables:	1
Number of figures:	9
Number of words in the Abstract:	253
Number of words in the Introduction:	800
Number of words in Materials and Methods:	2406
Number of words in Results:	1426
Number of words in Discussion:	1528
Number of References:	42

List of non-standard abbreviations.

ARA-C, cytosine β-D-arabinofuranoside; BAPTA-AM, 1,2-Bis(2-amino-5-methylphenoxy)ethane-N,N,N',N'-tetraacetic acid tetrakis(acetoxymethyl) ester; BHT, butylated hydroxytoluene; BSO, L-buthionine (S,R) sulfoximine; CGN, cerebellar granule neurons; CNQX, 6-cyano-7-nitroquinoxaline-2,3-dione disodium; DomA, domoic acid; DCFH$_2$-DA, 2,7'-dichlorofluorescin diacetate; DCF, 2,7'-dichlorofluorescein; DMSO, dimethylsulfoxide; DTT, dithiothreitol; EDTA, ethylenediamine-tetraacetic acid disodium salt; EGTA, ethylene glycol-bis(2-aminoethylether)-N,N,N′,N′-tetraacetic acid; FBS, fetal bovine serum; GCLC, glutamate

2

cysteine ligase catalytic subunit; GCLM, glutamate cysteine ligase modifier subunit;

γ–GT, gamma-glutamyltranspeptidase; GSH, glutathione; GSHEE, glutathione

ethylester; KA, kainic acid; MBB, monobromobimane; MK-801, (5R,10S)-(+)-5-

Methyl-10,11-dihydro-5H-dibenzo[*a,d*]cyclohepten-5,10-imine hydrogen maleate

; MSA, methanesulfonic acid; MTT, 3-(4,5- dimethylthiazol-2-yl)-2,5

diphenyltetrazolium bromide; NBQX, 2,3-dihydroxy-6-nitro-sulfamoylbenzo [*f*]

quinoxaline; NDA, naphthalene dicarboxaldehyde; NMDA, *N*-methyl-D-aspartate; PBN,

α -phenyl-N-tert-butyl-nitrone; PMSF, phenylmethylsulfonylfluoride; SSA, 5-

sulfosalicylic acid; SOD, superoxide dismutase; TCEP, tris (2-carboxyethyl)-phosphine

hydrochloride.

Abstract

This study investigated the role of cellular antioxidant defense mechanisms in modulating the neurotoxicity of domoic acid (DomA), by utilizing cerebellar granule neurons (CGN) from mice lacking the modifier subunit of glutamate-cysteine ligase (Gclm). Glutamate-cysteine ligase (Gcl) catalyzes the first and rate-limiting step in glutathione (GSH) biosynthesis. CGN from *Gclm* (-/-) mice have very low levels of GSH, and are ten fold more sensitive to DomA induced toxicity than CGN from *Gclm* (+/+) mice. GSH ethyl ester decreased, while the Gcl inhibitor buthionine sulfoximine increased, DomA toxicity. Antagonists of AMPA/kainate receptors and of NMDA receptors blocked DomA toxicity, and NMDA receptors were activated by DomA-induced L-glutamate release. The differential susceptibility of CGN to DomA toxicity was not due to a differential expression of ionotropic glutamate receptors, as evidenced by similar calcium responses and L-glutamate release in the two genotypes. A calcium chelator and several antioxidants antagonized DomA-induced toxicity. DomA caused a rapid decrease in cellular GSH, which preceded toxicity, and was primarily due to DomA-induced GSH efflux. DomA also caused an increase in oxidative stress as indicated by increases in reactive oxygen species and lipid peroxidation, which was subsequent to GSH efflux. Astrocytes from both genotypes were resistant to DomA toxicity, a diminished calcium response to DomA, and a lack of DomA-induced L-glutamate release. Because polymorphisms in the *GCLM* gene in humans are associated with low GSH levels, such individuals, as well as others with genetic conditions or environmental exposures that lead to GSH deficiency, may be more susceptible to DomA induced neurotoxicity.

Introduction

In 1987 in Canada, over 200 people became acutely ill after ingesting mussels. The outbreak resulted in twenty hospitalizations and the death of four people. Clinical effects observed included gastrointestinal symptoms and memory loss, and for this reason the condition was termed amnesic shellfish poisoning (ASP; Jeffery et al., 2004). The causative agent was soon identified as domoic acid (DomA), a neuroexcitatory toxin whose source was traced to a bloom of the diatom *Pseudo-nitzschia* (Perl et al., 1990). Neuropathological studies revealed neuronal necrosis and astrocytosis, predominantly in the hippocampus and the amygdala (Teitelbaum et al., 1990), and the same pattern of neurotoxic damage was also seen in primates, rats and mice given DomA (Tryphonas et al., 1990; Strain and Tasker, 1991; Sobotka et al., 1996; Scallet et al., 1993). DomA is a structural analog of kainic acid (KA), an excitatory amino acid that exerts its neurotoxicity by activating the AMPA/KA subtype of glutamate receptors (Hampson and Manalo, 1998). The pattern of brain damage observed in humans and in animals following exposure to DomA, resembles that seen after administration of KA (Teitelbaum et al., 1990), and a comparison of DomA and KA effects in vitro and in vivo confirms that DomA acts via KA receptors, and is 3 to 20 fold more potent than KA itself (Stewart et al., 1990).

Evidence accumulated over the past several years indicates that activation of ionotropic glutamate receptors may be an important source of oxidative stress leading to selective neuronal damage (Coyle and Puttfarcken, 1993). Oxidative stress refers to the cytotoxic consequences of reactive oxygen species (ROS) which are generated as

byproducts of normal and aberrant metabolic processes that utilize molecular oxygen. The tripeptide glutathione (GSH) is a major player in cellular defense against ROS, because it nonenzymatically scavenges both singlet oxygen and hydroxyl radicals, and is utilized by glutathione peroxidase (GPX) and glutathione S-transferase (GST) to limit the levels of certain reactive aldehydes and peroxides within the cell. When ROS production exceeds the antioxidant defense capacity of the cell, oxidative stress ensues, leading to damage of DNA, proteins and membrane lipids.

In vivo and in vitro studies suggest that oxidative stress is involved in KA neurotoxicity. In rat cortex, KA was found to increase levels of ROS (Bondy and Lee, 1993). In cultured rat retinal neurons, KA produces free radicals (Dutrait et al., 1995), while in rat cerebellar granule cells, KA was shown to induce ROS formation and lipid peroxidation (Puttfarcken et al., 1993). Activation of KA in cortical neurons results in marked elevation of intracellular calcium, and this in turn causes oxygen radical production (Carriedo et al., 1998). Administration of KA to gerbils increases free radical formation and lipid peroxidation in the brain (Sun et al., 1992), while in rats KA increases mitochondrial superoxide production in the hippocampus (Liang et al., 2000). Various antioxidants have been shown to inhibit KA-induced increases in oxidative stress and neurotoxicity, both in vitro and in vivo (Puttfarcken et al., 1993; Cheng and Sun, 1994; Miyamoto and Coyle, 1990; Wang et al., 2003). Exposure of rat cerebellar granule cells to KA also causes a significant reduction of GSH levels, and addition of GSH ethylester (GSHEE) increases cellular GSH levels, quenches generation of ROS, and reduces the neurotoxicity of KA (Ceccon et al., 2000).

There is only limited information on a possible role of oxidative stress in the neurotoxicity of DomA. In rat cortex, DomA was found to increase levels of ROS (Bondy and Lee, 1993), and DomA-induced neuronal death was attenuated by the centrally acting antioxidant melatonin (Ananth et al., 2003). DomA has also been found to elevate cerebral levels of superoxide dismutase as a consequence to its ability to promote oxidative stress (Bose et al., 2002).

Given the paucity of available information, the present study was undertaken to characterize the role of oxidative stress and of cellular antioxidant defense mechanisms, in DomA-induced neurotoxicity. For this purpose, we utilized primary cerebellar neurons from *Gclm* (-/-) mice, which lack the modifier subunit of glutamate cysteine ligase, the first and rate-limiting step in the synthesis of GSH (Yang et al., 2002). In the absence of GCLM, the ability of glutamate cysteine ligase catalytic subunit (GCLC) to synthesize GSH is drastically reduced (Dalton et al., 2004). Indeed, GSH levels in liver, kidney, pancreas, erythrocytes and plasma of *Gclm* (-/-) mice are only 9-16% of those found in *Gclm* (+/+) animals (Yang et al., 2002). Furthermore, genetic polymorphisms in the human *GCLM* gene have been reported. In particular, a C588T polymorphism in the 5'-flanking region of the gene has been shown to be associated with low plasma levels of GSH (Nakamura et al., 2002). Thus, *Gclm* (-/-) mice may represent a useful model for investigating the effects of compromised GSH synthesis, as has been observed in humans having this polymorphism in *GCLM*.

Materials and methods

Materials. Neurobasal-A medium, fetal bovine serum, B27 MinusAO, Hank's balanced salt solution, GlutaMax, Dispase and gentamicin were from Invitrogen (Carlsbad, CA, USA). Domoic acid, poly-D-lysine, cytosine β-D-arabinofuranoside (ARA-C), MK-801, (5R,10S)-(+)-5-Methyl-10,11-dihydro-5H-dibenzo[*a,d*]cyclohepten-5,10-imine hydrogen maleate (MK-801), superoxide dismutase (SOD), L-buthionine-*(S,R)*-sulfoximine (BSO), butylated hydroxytoluene (BHT), horseradish peroxidase-conjugated anti-mouse IgG, mouse anti-ß-actin antibody, horseradish peroxidase-conjugated anti-rabbit IgG, N-ethylmorpholine, dimethylsulfoxide (DMSO), and 3-(4,5- dimethylthiazol-2-yl)-2,5 diphenyltetrazolium bromide (MTT) were from Sigma Chemical Co. (St. Louis, MO, USA). Monobromobimane (MBB) was from Chemicon (La Jolla,CA,USA) . Protease inhibitors were from Boehringer Mannheim (Indianapolis, IN, USA). 6-Cyano-7-nitroquinoxaline-2,3-dione disodium (CNQX), 2,3-dihydroxy-6-nitro-sulfamoylbenzo[*f*]quinoxaline (NBQX), and melatonin were from Tocris Cookson (Ellisville, MO, USA). The reagents for enhanced chemiluminescence were from Amersham (Arlington Heights, IL, USA). The dNTPs were from Roche Diagnostics (Indianapolis, IN, USA) while the Taq polymerase was from Qiagen Inc. (Valencia, CA, USA). Naphthalene dicarboxaldehyde (NDA) and 2,7'-dichlorofluorescin diacetate (DCF-DA) were from Molecular Probes (Eugene, OR, USA).Tris (2-carboxyethyl)-phosphine hydrochloride (TCEP) was from Pierce (Rockford, IL, USA). The C18 solid phase extraction column was from JT Baker (Phillipsburg, NJ, USA).

Generation of Gclm-null mice and genotyping. All procedures for animal use were in accordance with the National Institute of Health Guide for the Use and Care of

Laboratory Animals, and were approved by the University of Washington Animal Care

and Use Committee. *Gclm*-null [*Gclm* (-/-)] mice were derived by homologous

recombination techniques in mouse embryonic stem (ES) cells. The β-galactosidase /

neomycin phosphotransferase β-Geo) fusion gene, a gift from Dr. Phil Soriano (Fred

Hutchinson Cancer Research Center), was flanked with approximately 2 kb of the mouse

Gclm gene promoter (left arm) and 1.5 kb of the first intron (right arm). This construct

also contained a diphtheria toxin gene driven by a thymidine kinase promoter to select

against random integrants. After selection of transfected 129SV strain ES cells with

G418, surviving colonies were assessed for targeted integration (disruption of the 1st exon

with β-Geo) using PCR. ES cells with the proper PCR product length were then assessed

by restriction digestion and Southern blot analyses. ES cells from correctly targeted

clones were subsequently injected into C57BL/6 mouse blastocysts and transplanted into

pseudopregnant mice according to standard techniques. Chimeric male pups born from

these mothers were mated to C57BL/6 females. Black agouti offspring were screened for

the targeted allele. These heterozygotes were intercrossed to obtain *Gclm* (-/-) mice.

Upon generation of the *Gclm* (-/-) mice, they were then crossed onto a C57BL/6

background for at least 7 generations prior to experiments. To genotype pups, we

analyzed for the presence of both the native *Gclm* gene and β-Geo sequences in two

separate reaction mixtures. The reactions utilized the same *Gclm* upstream primer 5'-

GCC CGC TCG CCA TCT CTC-3' (1 nM), while the β-Geo sequence was detected with

the reverse primer 5'-CAG TTT GAG GGG ACG ACG ACA-3' (1.25 nM), and the

native *Gclm* sequence was detected with the reverse primer 5'-GTT GAG CAG GTT

CCC GGT CT-3' (0.5 nM). Reactions (20 µl total volume) contained 0.4 mM each

9

dNTP, 1 unit of Taq polymerase and 1x reaction buffer, and 0.8 M DMSO. The cycling

conditions were as follows: 94°C for 2 minutes, followed by 35 cycles of 94°C for 45

seconds, 60°C for 45 seconds and 72°C for 2 minutes, and a final extension at 72°C for 5

minutes. Amplicons were resolved by agarose gel electrophoresis and stained with

ethidium bromide. Of all mice genotyped, 28 % were *Gclm* (+/+), 46% were *Gclm* (+/-),

and 26% were *Gclm* (-/-); these numbers approximate the expected Mendelian

percentages of 25:50:25, and indicate that no embryonic lethality occurred as a result of

the *Gclm* targeting.

Cultures of cerebellar granule neurons. Cultures of cerebellar granule neurons (CGN)

were prepared from 7 day-old mice sacrificed by decapitation. Cerebella were rapidly

dissected from the brain in Hibernate A/B27, meninges were removed, and tissue was cut

into 2 mm cubes. The tissue matrix was loosened by treating with Hibernate A containing

3 mg/ml of dispase for 30 min at 37°C. The tissue pieces were allowed to settle for 5 min

and the pellet was resuspended in Hibernate A medium containing 10 % of fetal bovine

serum (FBS) and 0.01 mg/ml DNase, before being mechanically dissociated by trituration

using a long-stem Pasteur pipette. After dissociation the cell suspension was centrifuged

in a refrigerated centrifuge at 300 x g for 5 min. The cell pellet was resuspended in

complete growth medium consisting of Neurobasal A medium containing 1 mM

GlutaMax, penicillin (100 U/ml), streptomycin (100 mg/ml), and FBS (10%). A 50 μl

sample of resuspended cells was added to a same volume of solution of trypan blue

(0.04% in PBS) and the percentage of viable cells was determined in a hemacytometer.

To remove any glial cells, the cell suspension was pre-plated for 20 min. After two

preplating steps, a higher than 97-98% purity of granule cells was achieved according to

immunocytochemical criteria. The cells were seeded at a density of 1×10^6 cells/cm^2 in

Neurobasal A with 10 % FBS in humidified 95% air/5% CO_2 at 37 ^{o}C. After 24 hr the

medium was removed and substituted with fresh prewarmed Neurobasal A containing

B27 Minus AO. This medium supplement (B27 Minus AO) is a newly improved

formulation without antioxidants and provides a sensitive and powerful antioxidant-free

primary culture system.

Cultures of cerebellar astrocytes. Cerebellar astrocytes obtained from brains of 7-8 day

old mice were prepared according to a method described previously (Guizzetti et al.,

2003) with minor modifications. Cells were grown in Dulbecco's modified Eagle's

medium (DMEM) supplemented with 10% fetal bovine serum, penicillin and

streptomycin in humidified 95% air/5% CO_2 at 37 °C. After one week, cells were

dissociated with 0.25% trypsin and 0.1% DNase in Hank's balanced salt solution, and

subcultured in 6 or 24 well multiplates. Culture medium was changed twice weekly.

Cultures contained more than 95% astrocytes as assessed by immunostaining for glial

fibrillary acidic protein.

Immunoblotting analyses. Neurons were scraped in lysis buffer (Tris 50 mM, pH 7.5, 2

mM EDTA, 0.5 mM EGTA, 0.5 mM phenylmethylsulfonylfluoride (PMSF), 0.5 mM

dithiothreitol, 10 μg/ml leupeptin, and 2 μg/ml aprotinin, 1mM sodium orthovanadate, 1

mM NaF, 0.25% SDS). Whole homogenates were subjected to SDS-PAGE and

immunoblotting as previously described (Giordano et al., 2005), using rabbit antibodies

against Gclc or Gclm proteins (both diluted 1:1500) or mouse anti-β-actin antibody

(1:5000). After electrophoresis, proteins were transferred to PDVF membranes that were

incubated with the above antibodies. Membranes were rinsed in TBS and incubated with

horseradish peroxidase-conjugated anti-rabbit IgG for GCLC and GCLM, or with

horseradish peroxidase-conjugated anti-mouse IgG for actin at the appropriate dilutions

(1:5000 for anti-Gclm and Gclc, and 1:15000 for anti-actin antibodies).

Measurement of GSH levels. Total intracellular GSH levels were measured using the

following procedure. Neurons were homogenized in Locke's buffer and an aliquot was

taken to measure the protein concentration while a second aliquot was diluted (1:1) in

10% 5-sulfosalicylic acid (SSA). The SSA fraction was centrifuged at 12000 rpm for 5

min at 4 ºC and the supernatant was used for GSH determinations. Aliquots from the SSA

fraction were added to a black flat bottom 96 well plate and pH was adjusted to 7 with

0.2 M N-ethylmorpholine/0.02 M KOH. Oxidized glutathione was reduced by adding 10

µl of 10 mM tris (2-carboxyethyl)-phosphine hydrochloride (TCEP) for 15 min at room

temperature. The pH was then adjusted to 12.5 using 0.5N NaOH   before derivatizing

the samples with naphthalene dicarboxaldehyde (NDA; 10 mM for 30 min). Finally the

samples were analyzed on a spectrofluorometric plate reader (λ_{EX} 472 and λ_{EM}528 nm).

After incubation, the total amount of GSH in the sample was expressed as nmol/mg

protein determinated from a standard curve obtained by plotting known amounts of GSH

incubated in the same experimental conditions vs. fluorescence.

Measurement of intracellular GSSG/GSH ratio. Intracellular GSSG/GSH ratio was

assayed using monobromobimane (MBB) as previously reported (Thompson et al., 2000)

with modifications as follows: briefly, cells were collected and washed in 1 ml of

Locke's buffer (pH of 7.4) and centrifuged for 5 min at 300 x g. The supernatant was

discarded and the cell pellet resuspended in 150 µl of Locke's buffer. An aliquot of 50 µl

was taken to measure the protein level and determine cell viability (by trypan blue

exclusion) while a second aliquot was diluited (1:1) with 10 % SSA to avoid oxidation of

GSH and to induce cell lysis. Two aliquots containing the same amount of protein were

taken from each sample; one aliquot was reduced via addition of TCEP (10 µl, 10 mM)

to determine total glutathione, while to the second aliquot a volume of 10 µl of water was

added for 15 min at 4ºC to determine reduced glutathione. A volume of 20 µl of MBB

solution (12.5 mM) was added for 30 min. GSSG was calculated by subtracting reduced

glutathione (GSH) from total glutathione. To ensure that TCEP effectively reduced all of

the GSSG in the sample to GSH, known amounts of GSSG were added to the extract and

incubated in presence of TCEP. HPLC analysis indicated that other compounds present in

the extract did not consume TCEP, and that the levels of GSSG in control samples were

about 3% of total intracellular glutathione.   The values for GSH and GSSG were

calculated from the mean of triplicate runs for each sample. The coefficient of variation

(CV) for measurements of GSH and GSSG were 3.9% and 17.8 %, respectively.

Measurement of GSH efflux. GSH efflux from neurons was measured using a

modification of White et al., (1999). Samples of Locke's buffer (5 ml) from treated and

untreated CGN were reduced with 20 µl of TCEP (10 mM) for 20 min at RT, and then

derivatized with MBB (20 µl of 2.5mM solution) for 30 min in the dark. The pH was then

adjusted to 2.0 by adding 1 ml of 5 % of SSA. The samples were then concentrated on a

C18 solid phase extraction column using a vacuum manifold. MBB-Glutathione

conjugate was eluted from the column with 1 ml ice cold methanol. Finally 25 µl of the

eluate was analyzed by HPLC against known standards.

Cytotoxicity Assay. DomA, GSH ethyl ester, NBQX, CNQX, MK- 801, BAPTA-AM and

SOD were dissolved in Locke's solution, while BHT, PBN were dissolved in DMSO.

Cells were washed once with Locke's solution and DomA was added for 1 hr, while antioxidants or receptor antagonists were added 30 min before the DomA treatment. At the end of DomA exposure, cultures were washed twice with Locke's solution and returned to their culture conditioned medium for a further 24 hr. Cell survival was quantified by a colorimetric method utilizing the metabolic dye 3-(4,5- dimethylthiazol-2-yl)-2,5 diphenyltetrazolium bromide (MTT). Culture medium was removed and replaced with 500 µl /well of Locke's solution containing 2 mg/ml MTT. After incubation for 30 min at 37 °C, the MTT solution was removed and the formazan reaction product dissolved in 250 µl of DMSO. Absorbance was read at 570 nm, and the results expressed as percent viable cells relative to unexposed controls.

Assay of Reactive Oxygen Species formation. ROS formation was determined by fluorescence using 2,7'-dichlorofluorescin diacetate ($DCFH_2$-DA). $DCFH_2$-DA is readily taken up by cells and is subsequently de-esterified to $DCFH_2$ (relatively low fluorescence). $DCFH_2$ can be oxidized to dichlorofluorescein (DCF) by hydrogen peroxide, peroxynitrite and other ROS/RNS (Kooy et al., 1997; Oyama et al.,1994). In a typical experiment, cells were first washed with Locke's solution, and then preincubated for 30 min (37 °C) with $DCFH_2$-DA (50 nmol/mg cell protein) in Locke's solution. $DCFH_2$-DA was added from a stock solution in methanol. Cells were then washed with Locke's solution to remove extracellular $DCFH_2$-DA. After treatments (at 37°C), the incubation solution was removed, and 0.1 M KH_2PO_4 0.5% Triton X-100 (pH 7.2) was added for 10 min. Cell lysates were then scraped from the dish and the extract centrifuged (10 min at 12000 rpm). The supernatant was collected and the fluorescence was immediately read using a Perkin-Elmer spectrofluorimeter (excitation 488 nm, emission

14

525 nm). ROS formation was expressed as the amount of DCF formed utilizing a DCF standard curve (0.01-100 µM).

Fluorescence imaging of cytoplasmic free Ca^{2+} in single cells. CGN or astrocytes were loaded with the Ca^{2+}-sensitive fluorescent dye fluo-3/AM (3 μM for neurons and 10 μM for astrocytes) at 37°C for 60 min in culture medium. Cells were then washed and incubated for an additional 30 min in a fluo-3/AM-free Locke's buffer to remove extracellular traces of the dye and to complete intracellular de-esterification. The 35 mm plates were placed on the stage of an inverted microscope. In some cases, a Ca^{2+}-free condition was achieved in Ca^{2+}-free Locke's buffer containing 0.1 mM EGTA. The dye in the cytoplasmic portion of the cells was excited, and fluorescence images were captured at 20-s intervals by a MicroMax cooled CCD camera (Princeton Instruments, Trenton, NJ) using Metamorph software (Molecular Devices Corp.Sunnyvale, CA).

Measurement of lipid peroxidation. CGN were scraped in 20 mM phosphate buffer, pH 7.4, and aliquots were removed to determine the protein content. After addition of an antioxidant (BHT, 10 µM) to prevent sample oxidation, the homogenate was centrifuged at 3000xg for 10 min to remove large cell fragments. N-Methyl-2-phenylindole and methanesulfonic acid (MSA) were then added and the samples were incubated at 45 °C for 60 min and then centrifuged (5000 x g for 10 min) to obtain a clear supernatant. Absorbance of the supernatant was read at 586 nm. Preliminary experiments designed to characterize the assays used in the our study found that samples containing the growth medium without cerebellar granule cells produced a significant absorbance reading for the ROS and lipid peroxidation assays. These false signals are most likely due to various

components such as trace metals. For this reason, these experiments were performed in

Locke's solution.

Measurement of L-glutamate release. Exposure conditions in L-glutamate release studies

were identical to those used in the excitoxicity assay. Buffers from treated cells were

collected, and determination of L-glutamate was carried out using the GLN-kit (Sigma).

This kit is designed for the spectrophotometric measurement of L-glutamine and/or L-

glutamate via enzymatic deamination of L-glutamine and dehydrogenation of L-

glutamate with reduction of NAD^+ to NADH. The conversion of NAD^+ to NADH was

measured spectrophotometrically at 340 nm and is proportional to the amount of

glutamate that is oxidized.

Statistical Analysis. Data are expressed as the mean ± SD of at least three independent

experiments. Statistical analysis was performed by Student's t-test for paired samples, or

by one way ANOVA followed by a Bonferroni post-test.

Results

GSH levels in cultured neurons and astrocytes from *Gclm* (-/-), *Gclm* (+/-) and *Gclm* (+/+) mice. As expected, the Gclm protein is not present in CGN from *Gclm* (-/-) mice, whilst the Gclc protein level is increased (Fig. 1A). Gclm is known to bind to Gclc and change the catalytic characteristics of Gclc in vitro. Since Gclc alone (in a *Gclm* (-/-) mouse) is predicted to function poorly in synthesizing γ-glutamylcysteine, the very low levels of GSH found in both CGN and cerebellar astrocytes from *Gclm* (-/-) mice (Fig. 1B), is not surprising. Cells from *Gclm* (+/-) mice displayed GSH levels similar to those found in *Gclm* (+/+) mice (Fig.1B). The higher GSH levels found in cerebellar astrocytes compared to CGN are in agreement with a previous study (Huang and Philbert, 1995). Of note is that CGN, in contrast to other neuronal cell types, contain relatively high levels of GSH (Lowndes et al., 1994). Intracellular GSH content of CGN declined as a function of culture age (20-25% at DIV 12), in contrast to cerebellar astrocytes where it was constant with time (data not shown).

***Gclm* (-/-) cerebellar granule neurons are more sensitive than *Gclm* (+/+) cells to DomA induced neurotoxicity.** To test the hypothesis that CGN from *Gclm* (-/-) mice might be more sensitive to DomA-induced toxicity, cell viability was measured by the MTT reduction assay. The IC_{50} values for DomA were 3.4 ± 1.3 µM in *Gclm* (+/+) neurons, and 0.39 ± 0.3 µM in *Gclm* (-/-) neurons (p<0.01). These experiments, as well as those that followed all, were also carried out in CGN from *Gclm* (+/-) mice. Since no significant differences were found between *Gclm* (+/+) and *Gclm* (+/-) neurons in response to DomA (IC_{50} of DomA was 3.1 µM $\pm$ 1.1 for *Gclm* (+/-) neurons), results

17

obtained in *Gclm* (+/-) cells are not shown. DomA did not cause any loss of viability in cerebellar astrocytes (Fig. 2B), irrespective of genotype.

The differential toxicity of DomA in CGN from *Gclm* (+/+) and *Gclm* (-/-) mice was not due to a different expression of ionotropic glutamate receptors, as evidenced by a similar calcium response evoked by DomA in both cell types (Fig. 2C). On the other hand, the calcium response induced by DomA in cerebellar astrocytes was much smaller (Fig. 2C). In CGN, calcium increase evoked by DomA was antagonized by the kainate/AMPA receptor antagonist NBQX and by the NMDA receptor antagonist MK-801, while in astrocytes only NBQX was effective (Fig. 2D).

To investigate the role of GSH in the neurotoxicity of DomA, CGN were incubated with the GSH delivery agent GSH ethyl ester (GSHEE, 2.5 mM). This treatment significantly increased cellular GSH content by 30 min (Fig. 3A), and prevented the toxicity of DomA (Fig. 3B). Furthermore, when CGN from *Gclm* (+/+) mice were exposed to BSO (an irreversible inhibitor of Gcl) at 25 µM for 24 hr, the expected depletion of intracellular GSH occurred (from 12.43 ± 1.4 to 3.7 ± 2.1 nmol/mg protein, an amount roughly equivalent to that in *Gclm* (-/-) cells), and the toxicity of DomA was significantly increased (Fig. 3C). Note that under these conditions, *Gclm* (+/+) neurons are as sensitive to DomA as *Gclm* (-/-) cells (not treated with BSO).

Pharmacological analysis of DomA toxicity. To investigate the role of ionotropic glutamate receptors in DomA-induced cytotoxicity, *Gclm* (+/+) and *Gclm* (-/-) neurons were preincubated with different antagonists. In the presence of 10 µM NBQX, a concentration that would prevent the activation of AMPA and KA receptors (Sheardown

et al., 1990), DomA-induced toxicity was completely blocked (Fig. 4). Similar results were found with another AMPA/KA receptor antagonist, CNQX (10 µM), and with the NMDA receptor antagonist MK-801, indicating that DomA toxicity is mediated by both AMPA/KA and NMDA receptors in mouse CGN (Fig. 4). Furthermore, the calcium chelator BAPTA-AM also prevented DomA-induced toxicity (Fig. 4). To test the hypothesis that NMDA receptors may be activated as a consequence of DomA-stimulated release of endogenous L-glutamate, CGN were exposed to 10 µM DomA for 10 min and the incubation buffers assayed for the presence of L-glutamate. Results of L-glutamate measurements were normalized to total protein content to account for variations in the numbers of cells on the plate. Fig. 5 shows the efflux of L-glutamate after a 15 min DomA exposure in CGN (A) and cerebellar astrocytes (B). In CGN DomA increased L-glutamate release. This was completely prevented by NBQX, and attenuated by BAPTA-AM and MK-801. This suggests that DomA, through activation of non-NMDA receptors, induces the release of L-glutamate from CGN, and this L-glutamate, in turn, activates NMDA receptors, which promote further increases in L-glutamate efflux (Bermann and Murray, 1997). In contrast, DomA did not cause any release of L-glutamate from cerebellar astrocytes (Fig. 5B).

Antioxidants prevent DomA toxicity. To further investigate the role of oxidative stress in DomA-induced neurotoxicity, CGN were preincubated with antioxidants [phenyl- N-tert butylnitrone (PBN; 100 µM); superoxide dismutase (SOD; 100 U/ml); melatonin (200 µM); butylated hydroxytoluene (BHT; 100 µM)], followed by treatment with DomA. All compounds protected *Gclm* (+/+) and *Gclm* (-/-) neurons against DomA-

19

induced neurotoxicity (Fig. 6). The free radical spin trapping agent PBN was particularly

effective at preventing DomA-induced neurotoxicity, suggesting that the generation of

superoxide and free radicals might have a central role in DomA-induced cell death.

Effect of DomA on ROS production and lipid peroxidation. ROS production was

measured with the oxidant-sensitive fluorescent dye 2',7'-dichlorodihydrofluorescin

diacetate (DCFH$_2$-DA). DomA caused a significant time-, and concentration-dependent

increase in ROS production, with a maximal effect after 1 hr incubation (Fig.7A, B).

Production of ROS was significantly higher in *Gclm* (-/-) neurons (21.97 ± 1.26 pmol

DCF/mg protein) than in *Gclm* (+/+) neurons (10.23 ± 1.05 pmol DCF/mg protein) (p<

0.01). The AMPA/KA receptor antagonists NBQX and CNQX, and the NMDA receptor

antagonist MK-801, as well as BAPTA-AM, significantly attenuated the ROS production

induced by DomA (Fig. 7C). Antioxidants and GSHEE also inhibited DomA-induced

ROS formation (Fig. 7D). Thus, all compounds that inhibit DomA-induced cytotoxicity,

also reduce DomA-induced production of ROS.

The ability of DomA to induce lipid peroxidation was assessed by determining

changes in malondialdehyde (MDA) concentrations. A time-course experiment indicated

that the maximum increase in lipid peroxidation was present approximately 2 hr after

DomA exposure (not shown). DomA caused an increase in MDA levels, which was

significantly greater in CGN from *Gclm* (-/-) mice (Table 1). DomA-induced lipid

peroxidation was inhibited by GSHEE, NBQX and MK-801 (Table 1).

Effect of DomA on intracellular levels of GSH and GSSG, and on GSH efflux.

DomA caused a time-dependent loss of total cellular GSH in CGN (Fig. 8A). This decrease was prevented by ionotropic glutamate receptor antagonists, but not by antioxidants (Fig. 8B). Near maximal depletion of cellular GSH was observed after 1hr incubation with DomA, before any cytotoxicity is apparent (Fig. 8C).

Cellular GSH levels are thought to be determined by the rates of synthesis and loss of the tripeptide via oxidation, utilization in glutathione S-transferase mediated conjugation reactions, $\gamma-$ glutamyltranspeptidase ($\gamma-$GT) mediated amino acid transport, or by excretion. GSH depletion is commonly observed when cells are oxidatively stressed and can be detected by measurement of transient increases in intracellular glutathione disulfide (GSSG) content. Despite a massive and rapid GSH loss, there was only a modest increase in GSSG intracellular content upon exposure to DomA, which was prevented by NBQX and MK-801 (Fig. 9A). Declining GSH levels might result either from an increased efflux out of the cell or a reduced rate of synthesis. To discriminate between these two possibilities, GSH synthesis was blocked by BSO; this treatment decreased intracellular GSH levels by about 40-45 % after 6 hr (Fig. 9B). However, DomA induced a much more rapid drop in GSH levels (Fig. 9B). To determine whether GSH was being extruded from the CGN, the incubation medium was collected and derivatized with monobromobimane prior to analysis by HPLC. DomA caused an increase of net efflux of total GSH in *Gclm* (+/+) and *Gclm* (-/-) neurons, which was prevented by ionotropic glutamate receptor antagonists (Fig.9 C). Because extracellular GSH may be utilized by $\gamma-$GT, the experiments were carried out with acivicin (0.2 mM), an inhibitor of this enzyme. Similar to earlier studies (Wallin et al., 1999), we found that

21

inhibition of γ–GT activity increased the recovery of GSH in the medium. A time-course

experiment shows that efflux of glutathione from DomA-treated cells begins after 15 min

of DomA treatment (Fig. 9D), concomitant with the decrease in intracellular GSH (Fig.

8A). Efflux of GSH and the decrease in intracellular GSH precede the production of ROS

induced by DomA (Fig. 7A).

Discussion

Although DomA is a well-known neurotoxin, the biochemical mechanisms involved in its neurotoxic effect are still elusive. Because of its structural similarity to KA, DomA is believed to exert its neurotoxicity by binding to, and activating a subclass of non-NMDA excitatory amino acid receptors, the AMPA/KA receptors.

KA neurotoxicity has been suggested to be mediated by increased oxidative stress (Bondy and Lee, 1993; Puttfarcken et al., 1993; Carriedo et al., 1998; Sun et al., 1992; Liang et al., 2000). In this study we investigated the role of GSH in modulating the toxicity of DomA. For this purpose we utilized a genetic model of GSH deficiency, i.e. CGN derived from mice with compromised GSH synthesis, due to the lack of the modifier subunit of glutamate-cysteine ligase (*Gclm* -/- mice). Our results indicate that GSH plays a critical role in modulating the neurotoxicity of DomA, and this is supported by various lines of evidence. First, *Gclm* (-/-) neurons, which have a much lower levels of GSH, are ten-fold more sensitive to DomA toxicity then CGN from *Gclm* (+/+) mice. Second, the membrane permeant GSH delivery agent GSHEE restored intracellular GSH levels in *Gclm* (-/-) neurons, and this afforded protection against DomA induced toxicity. Third, depletion of GSH by L-buthionine sulfoximine in *Gclm* (+/+) CGN rendered them as sensitive to DomA as *Gclm* (-/-) neurons. The different susceptibility of CGN from the two mouse strains was not due to different expression of ionotropic glutamate receptors, as suggested by the fact that DomA induced an identical calcium response in both *Gclm* (+/+) and *Gclm* (-/-) neurons.

Neurotoxicity of DomA was antagonized by AMPA/KA receptor antagonists and by an antagonist of NMDA receptors. The involvement of NMDA receptors is most

likely due to DomA-induced release of L-glutamate, as previously suggested (Berman and Murray, 1997; Berman et al., 2002). The finding that MK-801 inhibited DomA-induced L-glutamate release suggests that activation of NMDA receptors by the released L-glutamate further promotes L-glutamate release. It should be noted that DomA-induced L-glutamate release was similar in *Gclm* (+/+) and (-/-) neurons, indicating that this process does not explain their differential susceptibility to DomA toxicity.

DomA-induced neurotoxicity was also prevented by several antioxidants, in both *Gclm* (+/+) and (-/-) neurons. A particularly effective antioxidant was the free radicals spin trapping agent PBN, suggesting that superoxide and free radical may be generated by DomA in CGN. Indeed, DomA caused a time- and concentration dependent increase in ROS, which was significantly higher in CGN from *Gclm* (-/-) mice. Such DomA-induced increases in ROS were antagonized by AMPA/KA and NMDA receptor antagonists, by GSH ethyl ester, and by antioxidants. Since one consequence of increased ROS production is an increase in lipid peroxidation, we determined whether the latter was increased by DomA. This was indeed the case, with a greater increase in malondialdehyde (MDA) production in *Gclm* (-/-) neurons compared with their wild-type counterparts.

In order to probe the mechanism underlying the increased ROS production induced by DomA, we investigated the effect of DomA on intracellular GSH levels. In both *Gclm* (+/+) and *Gclm* (-/-) neurons, DomA induced a time-dependent decrease of intracellular GSH. This effect was not due to inhibition of GSH synthesis by DomA, as suggested by a comparison of the time-courses of GSH decline upon exposure to DomA and BSO. Alternative explanations for the DomA-induced GSH loss would be oxidation

to GSSG, or its release from the cell. DomA caused only a modest increase in intracellular GSSG content. However, it caused a highly significant increase in GSH efflux from both *Gclm* (+/+) and *Gclm* (-/-) neurons.

The calcium chelator BAPTA-AM also antagonized DomA-induced toxicity, L-glutamate release and GSH efflux, suggesting an involvement of calcium in these effects. A comparison of the time-course of DomA-induced effects in CGN suggests the following sequence of events in DomA-mediated neurotoxicity. By activating AMPA/KA receptors, DomA causes an increase in $[Ca]_i$ which then results in a release of L-glutamate. This released L-glutamate in turn activates NMDA receptors and promotes further L-glutamate release. This combined action causes a rapid accumulation in $[Ca]_i$, promotes GSH efflux and a concomitant decrease in intracellular GSH. High $[Ca]_i$ and low intracellular GSH leads to production of ROS, which are probably of mitochondrial origin (Carriedo et al., 1998). Because there is insufficient GSH to scavenge the ROS, there is an increase in lipid peroxidation, and this contributes to cell death. In CGN from *Gclm* (-/-) mice, initial responses to DomA (increase in intracellular calcium and L-glutamate release) are identical to those observed in GCN from wild type animals. Similarly, GSH efflux and a decrease of GSH levels upon DomA stimulation are also observed. However, since these latter effects cause a further reduction in GSH from an already low basal, ROS levels are higher and promote higher lipid peroxidation and enhanced toxicity in Gclm (-/-) CGN.

These findings show that by activating AMPA/KA receptors (directly) and NMDA receptors (indirectly), the extent of DomA-induced neuronal death is dictated by intracellular GSH levels. DomA-induced oxidative stress is significantly more

pronounced in *Gclm* (-/-) neurons, which have very low GSH levels. Thus, low levels of

GSH, due either to genetic manipulation and/or to DomA-induced GSH efflux, may

mediate DomA –induced neuronal cell death. Indeed, GSH depletion has been shown to

cause mitochondrial dysfunction and activation of 12-lipoxygenase, resulting in the

production of peroxides and the activation of neuronal magnesium-dependent

sphingomyelinase and the production of ceramide (Liu et al., 1997). DomA-induced GSH

efflux precedes any permeability of the cell membrane, and may be explained by

induction of a specific GSH transporter, such as seen with NMDA (Wallin et al., 1999).

However, the exact mechanism of DomA –induced GSH efflux still needs to be

investigated.

Additional evidence that GSH levels play a central role in modulating DomA

toxicity is that depletion of GSH by BSO rendered CGN from *Gclm* (+/+) mice as

sensitive as CGN from *Gclm* (-/-) mice. Conversely, increasing GSH levels in *Gclm* (-/-)

neurons by means of GSHEE administration rendered them as resistant as their wild-type

counterparts. This finding differs from that reported in mouse fibroblasts exposed to

H_2O_2 (Yang et al., 2002). In that case, depletion of GSH with the GST substrate phorone

increased the sensitivity of *Gclm* (+/+) cells to H_2O_2, but not to the extent observed in

Gclm (-/-) fibroblasts. Conversely, GSHEE afforded only partial protection against H_2O_2

in *Gclm* (-/-) cells. It was suggested that it is not the level of GSH itself, but the GSH

synthetic potential, that may be the major determinant for protecting against oxidative

insult (Yang et al., 2002). The different cell type, the use of BSO instead of phorone, and

the ability of DomA to induce GSH efflux may be reasons for the observed differences

between our results and those of Yang et al. (2002).

A relatively common C588T polymorphism has been discovered in the 5'-flanking region of the *GCLM* gene (Nakamura et al., 2002). Individuals carrying the T allele have lower promoter activity in a luciferase reporter gene assay in response to oxidants, and significantly lower plasma GSH levels (Nakamura et al., 2002). These individuals are also at higher risk for myocardial infarction, and present impairments in nitric oxide-mediated coronary vasomotor function (Nakamura et al., 2002; 2003). It would be interesting to know if individuals carrying the T allele may also display lower GSH levels in the CNS, and thus may be more susceptible to DomA-induced neurotoxicity. Evidence suggests that non-human primates may be more sensitive than rodents to DomA-induced neurotoxicity, and neonatal animals may be more susceptible than adults (Jeffery et al., 2004). Our results suggest that individuals with *GCLM* polymorphisms, or other mutations leading to decreased GSH levels (Dalton et al., 2004), would display an even enhanced sensitivity to DomA neurotoxicity.

An additional interesting finding of our studies relates to the effects of DomA in cerebellar astrocytes. The presence of ionotropic glutamate receptors in astrocytes is still the subject of debate (Seifert and Steinhauser, 2001). Clear evidence for a functional expression of KA receptors in astrocytes is lacking. However, electrophysiological and biochemical responses to KA have been reported, possibly mediated by AMPA receptors (Farr et al., 1999; Telgkamp et al., 1996). Furthermore, whether NMDA receptors exist in astrocytes is also controversial (Ziak et al., 1998; Seifert and Steihouser, 2001). Our results clearly indicate that cerebellar astrocytes are resistant to DomA toxicity, and this holds true even for astrocytes from *Gclm* (-/-) mice, which have very low levels of GSH. Incubation of astrocytes with DomA elicited a modest increase in $[Ca^{2+}]_i$ compared

to that observed in CGN, and the response did not differ between the two genotypes. This small increase in $[Ca^{2+}]_i$ was due only to activation of AMPA/KA receptors, but was not sufficient to elicit L-glutamate release and possible ensuing activation of NMDA receptors. The lack of a robust calcium response in astrocytes would explain their resistance to DomA toxicity, even in the presence of low GSH. Furthermore, no release of L-glutamate was observed in astrocytes in response to DomA. This finding would also support the suggestion that activation of NMDA receptors by AMPA/KA receptor-mediated stimulation of glutamate release is the initial more relevant step in DomA neurotoxicity (Berman et al., 2002).

Acknowledgments

References

Ananth C, Gopalakrishnakone P, Kaur C (2003) Protective role of melatonin in domoic acid-induced neuronal damage in the hippocampus of adult rats. *Hippocampus* **13**:375-87.

Berman FW, LePage KT, Murray TF (2002) Domoic acid neurotoxicity in cultured cerebellar granule neurons is controlled preferentially by the NMDA receptor Ca(2+) influx pathway. *Brain Res* **924**:20-9.

Berman FW, Murray TF (1997) Domoic acid neurotoxicity in cultured cerebellar granule neurons is mediated predominantly by NMDA receptors that are activated as a consequence of excitatory amino acid release. *J Neurochem* **69**:693-703.

Bondy SC, Lee DK (1993) Oxidative stress induced by glutamate receptor agonists. *Brain Res* **610**:229-33.

Bose R., Schnell C.L., Pinsky C., Zitko V. (1992) Effects of excitotoxins on free radicals indices in mouse brain. *Toxicol Lett* **60**:211-9.

Carriedo SG, Yin HZ, Sensi SL, Weiss JH (1998) Rapid Ca2+ entry through Ca2+-permeable AMPA/Kainate channels triggers marked intracellular Ca2+ rises and consequent oxygen radical production. *J Neurosci* **18**:7727-38.

Ceccon M, Giusti P, Facci L, Borin G, Imbesi M, Floreani M, Skaper SD (2000) Intracellular glutathione levels determine cerebellar granule neuron sensitivity to excitotoxic injury by kainic acid. *Brain Res* **17**:83-9.

Cheng Y, Sun AY (1994) Oxidative mechanisms involved in kainate-induced cytotoxicity in cortical neurons. *Neurochem Res* **19**:1557-64.

Coyle JT, Puttfarcken P (1993) Oxidative stress, glutamate, and neurodegenerative disorders. *Science* **262**:689-95.

Dalton TP, Chen Y, Schneider SN, Nebert DW, Shertzer HG (2004) Genetically altered mice to evaluate glutathione homeostasis in health and disease. *Free Radic Biol Med* **37**:1511-26.

Dutrait N, Culcasi M, Cazevieille C, Pietri S, Tordo P, Bonne C, Muller A (1995) Calcium-dependent free radical generation in cultured retinal neurons injured by kainate. *Neurosci Lett* **198**:13-6.

Fan D, Grooms SY, Araneda RC, Johnson AB, Dobrenis K, Kessler JA, Zukin RS (1999) AMPA receptor protein expression and function in astrocytes cultured from hippocampus. *J Neurosci Res* **57**:557-71.

Giordano G, Sanchez-Perez AM, Burgal M, Montoliu C, Costa LG, Felipo V (2005) Chronic exposure to ammonia induces isoform-selective alterations in the intracellular distribution and NMDA receptor-mediated translocation of protein kinase C in cerebellar neurons in culture. *J Neurochem* **9**:143-57.

Guizzetti M, Bordi F, Dieguez-Acuna FJ, Vitalone A, Madia F, Woods JS, Costa LG (2003) Nuclear factor kappaB activation by muscarinic receptors in astroglial cells: effect of ethanol. *Neuroscience* **120**:941-50.

Hampson DR, Manalo JL (1998) The activation of glutamate receptors by kainic acid and domoic acid. *Nat Toxins* **6**:153-8. Review.

Huang J, Philbert MA (1995) Distribution of glutathione and glutathione-related enzyme systems in mitochondria and cytosol of cultured cerebellar astrocytes and granule cells. *Brain Res* **22**:16-22.

Jeffery B, Barlow T, Moizer K, Paul S, Boyle C (2004) Amnesic shellfish poison. *Food Chem Toxicol* **42**:545-57.

Kooy NW, Royall JA, Ischiropoulos H (1997) Oxidation of 2',7'-dichlorofluorescin by peroxynitrite. *Free Radic Res*. **27**:245-54.

Liang LP, Ho YS, Patel M (2000) Mitochondrial superoxide production in kainate-induced hippocampal damage. *Neuroscience* **101**:563-70.

Liu B, Obeid LM, Hannun YA (1997) Sphingomyelinases in cell regulation. *Semin Cell Dev Biol* **8**:311-322.

Lowndes HE, Beiswanger CM, Philbert MA, Reuhl KR. (1994) Substrates for neural metabolism of xenobiotics in adult and developing brain. *Neurotoxicology* **15:**61-73. Review.

Miyamoto M, Coyle JT (1990) Idebenone attenuates neuronal degeneration induced by intrastriatal injection of excitotoxins. *Exp Neurol* **108**:38-45.

Nakamura S, Kugiyama K, Sugiyama S, Miyamoto S, Koide S, Fukushima H, Honda O, Yoshimura M, Ogawa H (2002) Polymorphism in the 5'-flanking region of human glutamate-cysteine ligase modifier subunit gene is associated with myocardial infarction. *Circulation* **105**:2968-73.

Nakamura S, Sugiyama S, Fujioka D, Kawabata K, Ogawa H, Kugiyama K (2003). Polymorphism in glutamate-cysteine ligase modifier subunit gene is associated with impairment of nitric oxide-mediated coronary vasomotor function. *Circulation* **108**:1425-7.

Oyama Y, Hayashi A, Ueha T, Maekawa K (1994) Characterization of 2',7'-dichlorofluorescin fluorescence in dissociated mammalian brain neurons: estimation on intracellular content of hydrogen peroxide. *Brain Res* **635**:113-7.

Perl TM, Bedard L, Kosatsky T, Hockin JC, Todd EC, Remis RS (1990) An outbreak of toxic encephalopathy caused by eating mussels contaminated with domoic acid. *N Engl J Med* **322**:1775-80

Puttfarcken PS, Getz RL, Coyle JT (1993) Kainic acid-induced lipid peroxidation: protection with butylated hydroxytoluene and U78517F in primary cultures of cerebellar granule cells. *Brain Res* **624**:223-32.

Scallet AC, Binienda Z, Caputo FA, Hall S, Paule MG, Rountree RL, Schmued L, Sobotka T, Slikker W Jr (1993) Domoic acid-treated cynomolgus monkeys (M. fascicularis): effects of dose on hippocampal neuronal and terminal degeneration. *Brain Res* **627**:307-13.

Seifert G, Steinhauser C (2001) Ionotropic glutamate receptors in astrocytes. *Prog Brain Res* **132**:287-99. Review.

Sheardown MJ, Nielsen EO, Hansen AJ, Jacobsen P, Honore T. (1990) 2,3-Dihydroxy-6-nitro-7-sulfamoyl-benzo(F) quinoxaline: a neuroprotectant for cerebral ischemia. *Science* **247**:571-4.

Sobotka TJ, Brown R, Quander DY, Jackson R, Smith M, Long SA, Barton CN, Rountree RL, Hall S, Eilers P, Johannessen JN, Scallet AC (1996) Domoic acid: neurobehavioral and neurohistological effects of low-dose exposure in adult rats. *Neurotoxicol Teratol* **18**:659-70.

Stewart GR, Zorumski CF, Price MT, Olney JW (1990) Domoic acid: a dementia-inducing excitotoxic food poison with kainic acid receptor specificity. *Exp Neurol* **110**:127-38.

Strain SM, Tasker RA (1991) Hippocampal damage produced by systemic injections of domoic acid in mice. *Neuroscience* **44**:343-52.

Sun AY, Cheng Y, Bu Q, Oldfield F (1992) The biochemical mechanisms of the excitotoxicity of kainic acid. Free radical formation. *Mol Chem Neuropathol* **17**:51-63.

Teitelbaum JS, Zatorre RJ, Carpenter S, Gendron D, Evans AC, Gjedde A, Cashman NR (1990) Neurologic sequelae of domoic acid intoxication due to the ingestion of contaminated mussels. *N Engl J Med* **322**:1781-7.

Telgkamp P, Backus KH, Deitmer JW (1996) Blockade of AMPA receptors by nickel in cultured rat astrocytes. *Glia* **16**:140-6.

Thompson SA, White CC, Krejsa CM, Eaton DL, Kavanagh TJ. (2000) Modulation of glutathione and glutamate-L-cysteine ligase by methylmercury during mouse development. *Toxicol Sci*. **57**:141-6.

Tryphonas L, Truelove J, Todd E, Nera E, Iverson F (1990) Experimental oral toxicity of domoic acid in cynomolgus monkeys (Macaca fascicularis) and rats. Preliminary investigations. *Food Chem Toxicol* **28**:707-15.

Wallin C, Weber SG, Sandberg M (1999) Glutathione efflux induced by NMDA and kainate: implications in neurotoxicity? *J Neurochem* **73**:1566-72.

Wang H, Cheng E, Brooke S, Chang P, Sapolsky R (2003) Over-expression of antioxidant enzymes protects cultured hippocampal and cortical neurons from necrotic insults. *J Neurochem* **87**:1527-34.

White CC, Krejsa CM, DL Eaton, and Kavanagh TJ (1999) HPLC-Based assay for enzyme of glutathione biosynthesis. *Current Protocols in Toxicology* 6.5.1-6.5.14

Yang Y, Dieter MZ, Chen Y, Shertzer HG, Nebert DW, Dalton TP (2002) Initial characterization of the glutamate-cysteine ligase modifier subunit *Gclm*(-/-) knockout mouse. Novel model system for a severely compromised oxidative stress response. *J Biol Chem* **277**:49446-52

Ziak D, Chvatal A, Sykova E (1998) Glutamate-, kainate- and NMDA-evoked membrane

currents in identified glial cells in rat spinal cord slice. *Physiol Res* **47**:365-75.

Footnotes to the title

Dr. Lucio G. Costa. Department of Environmental and Occupational Health Sciences University of Washington, 4225 Roosevelt Way NE, Suite 100. Seattle, WA 98105
Email: lgcosta@u.washington.edu

Legend to Figures

Fig 1. A. Western blot analysis of Gclm and Gclc proteins in mouse CGN. B. GSH levels in CGN and cerebellar astrocytes from *Gclm* (+/+), *Gclm* (+/-) and *Gclm* (-/-) mice. Results represent the mean (± SD) of at least three experiments. *Significantly different from *Gclm* (+/+) (p < 0.01).

Fig. 2. Effect of DomA on viability and calcium response in CGN and cerebellar astrocytes. CGN (A) and cerebellar astrocytes (B) from mice of both *Gclm* (+/+) and (-/-) genotypes were treated with DomA, and cell viability was assessed after 24 hr by MTT reduction. Data are presented as percentage of untreated CGN taken as control, and represent the mean (± SD) of at least three experiments. All points in *Gclm* (-/-) CGN are significantly different from *Gclm* (+/+) CGN (p< 0.01). In (C), the effects of DomA (1 and 10 μM) on intracellular [Ca^{2+}] levels in CGN and astrocytes of both *Gclm* (+/+) and (-/-) genotypes, as measured by fluo-3 fluorescence, are shown. The effects of NBQX (10 μM) and MK-801 (5 μM) on intracellular [Ca^{2+}] increase induced by 10 μM of DomA in CGN and cerebellar astrocytes from *Gclm* (+/+) mice are shown in D. Data are expressed as arbitrary units of fluorescence and represent the mean ± SD of three experiments. *Significantly different from control astrocytes (p < 0.05). **Significantly different from control CGN (p < 0.01).

Fig. 3. A. Total GSH levels in *Gclm* (+/+) and *Gclm* (-/-) CGN after exposure to 2.5 mM GSH ethylester (GSHEE) for different times. Data are expressed as nmol of glutathione per mg of protein, and represent the mean (± SD) of at least three experiments. *

Significantly different from control (p < 0.01). B. Toxicity of DomA (10 µM) following a

30 min pretreatment with 2.5 mM GSHEE, as assessed by the MTT reduction assay. Data

represent the mean (± SD) of at least three experiments. *Significantly different from

DomA-treated cells of the same genotype (p < 0.01). C. Effect of BSO pretreatment on

DomA-induced toxicity. CGN from *Gclm* (+/+) mice were pretreated with BSO (25 µM)

for 24 hr and then challenged with DomA (10 µM). * Significantly different from *Gclm*

(+/+) CGN in the absence of BSO (p < 0.05). Data represent the mean (± SD) of at least

three experiments.

Fig. 4. Effects of NBQX (10 µM), CNQX (50 µM), MK-801 (5 µM) and BAPTA-AM

(5 µM) on DomA (10 µM)-induced toxicity in CGN. Results are expressed as percent of

untreated CGN, and represent the mean (± SD) of at least three

experiments.*Significantly different from DomA-treated CGN (p < 0.01).

Fig. 5. Efflux of L-glutamate from CGN (A) and cerebellar astrocytes (B) exposed to

DomA (10 µM; 15 min) alone, or in combination with either 10 µM NBQX, 5 µM MK-

801 or 5 µM BAPTA-AM. Results are expressed as percent of control for each genotype.

Data represent the mean (± SD) of at least three experiments. *Significantly different

from control (p<0.01)

Fig 6. Antioxidants protect CGN from DomA-induced neurotoxicity. CGN of both

genotypes were exposed to 10 µM DomA, alone or in combination with 100 µM PBN,

100 U/ml SOD, 200 µM melatonin, or 100 µM BHT at 37 ºC for 60 min. Cell survival

was quantified 24 h later by the MTT assay. The protection afforded by all antioxidants in preventing DomA-induced toxicity was statistically significant in both genotypes ($p < 0.01$). Data represent the mean ($\pm$ SD) of at least three experiments.

Fig. 7. A. Time-course of ROS production following treatment with 10 µM DomA. Results represent the mean ($\pm$ SD) of at least three experiments. *Significantly different from the respective control ($p < 0.05$). B. Concentration-response effect of DomA on ROS levels, measured at 60 min. Results represent the mean ($\pm$ SD) of at least three experiments. *Significantly different from control ($p < 0.05$). (C,D) Effect of glutamate receptor antagonists (C) and antioxidants (D) on DomA-induced ROS generation in CGN. Cells of both genotypes were incubated with 10 µM DomA, alone or in combination with either 5 µM MK-801, 10 µM NBQX, 10 µM CNQX, 5 µM BAPTA-AM, 100 µM of PBN, 100 U/ml SOD, 200 µM melatonin or 100 µM BHT. Results represent the mean ($\pm$ SD) of at least three experiments. *Significantly different from untreated cells of the same genotype ($p<0.05$).

Fig. 8. A. Time-course of DomA-induced decrease of cellular GSH in CGN. Results represent the mean ($\pm$ SD) of at least three experiments. *Significantly different from the respective control ($p < 0.01$). B. Effect of NBQX (10 µM), MK-801 (5 µM), PBN (100 µM) and SOD (100 U/ml) on DomA (10 µM)-induced GSH decrease in CGN. Results represent the mean ($\pm$ SD) of at least three experiments. *Significantly different from control CGN ($p < 0.01$). C. Time-course of DomA (10 µM) –induced cytotoxicity (MTT assay) and decrease in intracellular GSH levels in CGN from *Gclm* (+/+) mice. Result

represent the mean (± SD) of at least three experiments. *Significantly different from

control (p < 0.01).

Fig. 9. A. Effect of DomA (10 µM, 1hr), alone or in combination with 10 µM NBQX or

5 µM MK-801, on intracellular GSSG levels in CGN. GSSG is expressed as percent of

total glutathione (GSH+GSSG). *Significantly different from control (p < 0.01).

**Significantly different from control (p < 0.005). B. Time-course of GSH loss after

treatment with 25 µM BSO or 10 µM DomA in *Gclm* (+/+) CGN. Total glutathione

content was assessed by the NDA assay. *Significantly different from control (p < 0.05).

C. Effect of DomA (10 µM, 1hr), alone or in combination with 10 µM NBQX or 5 µM

MK-801, on GSH efflux in CGN. Results are expressed as percent of efflux of GSH

present in untreated *Gclm* (+/+) CGN. *Significantly different from the respective control

(p < 0.005). D. Time course of DomA (10 µM)-induced GSH efflux in *Gclm* (+/+) CGN.

Results are expressed as percent of efflux of GSH present in untreated *Gclm* (+/+) CGN.

*Significantly different from control (p < 0.05). **Significantly different from control (p

< 0.01).

TABLE 1

Table 1. **DomA-induced lipid peroxidation in CGN**

	MDA (arbitrary units/μg protein)	
	Gclm (+/+)	*Gclm (-/-)*
Control	52 ± 7.0	91 ± 18.4*
DomA 10 μM	126 ± 12.7*	231 ± 20.5**
DomA + NBQX 10μM	72 ± 8.2	113 ± 6.0
DomA + MK801 5 μM	79 ± 11.6	129 ± 5.1
DomA +GSHEE 2.5 mM	66 ± 14.1	94 ± 21.5

CGN of both genotypes were exposed to 10 μM DomA, alone or in combination with the indicated compounds and incubated at 37 ºC for 60 min. After 1 hr recovery in maintenance growth medium, lipid peroxidation was assessed by the malondialdehyde (MDA) assay. Results represent the mean (± SD) of at least three experiments. *Significantly different from untreated *Gclm* (+/+) neurons ($p < 0.05$). ** Significantly different from untreated *Gclm* (-/-) neurons ($p < 0.01$).
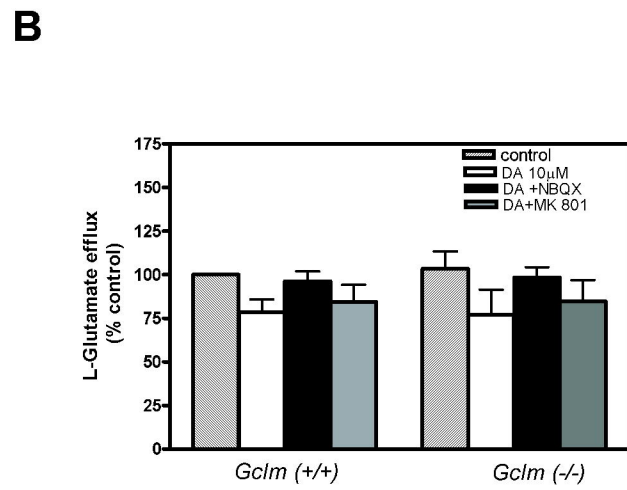
42

FIGURE 1

A

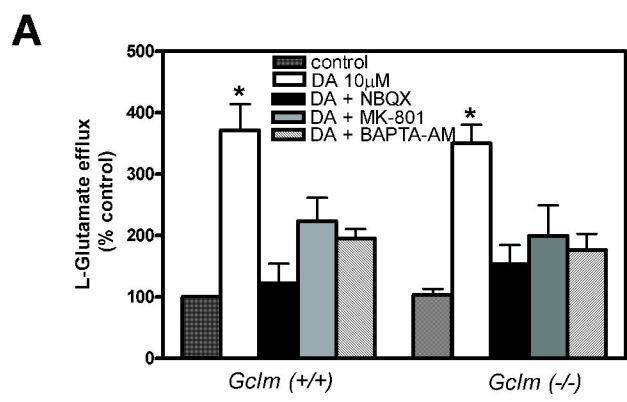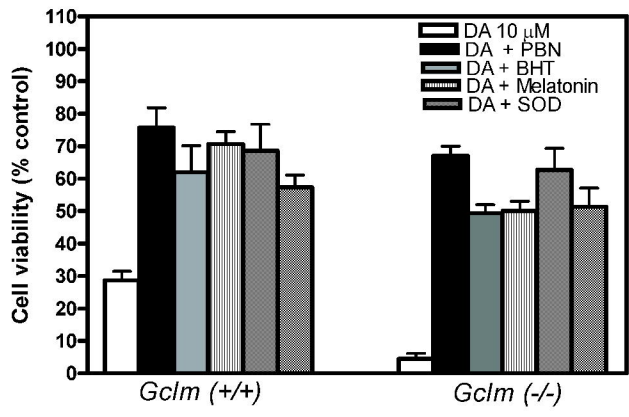Cerebellar granule cells
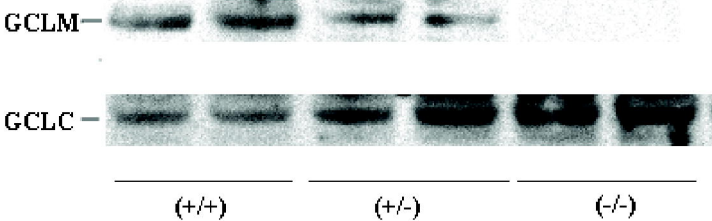
B
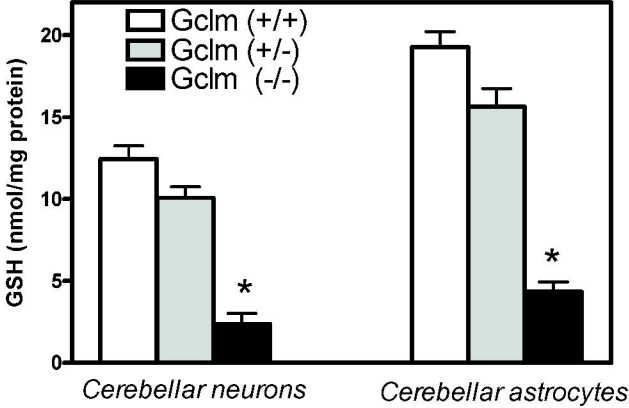
FIGURE 2
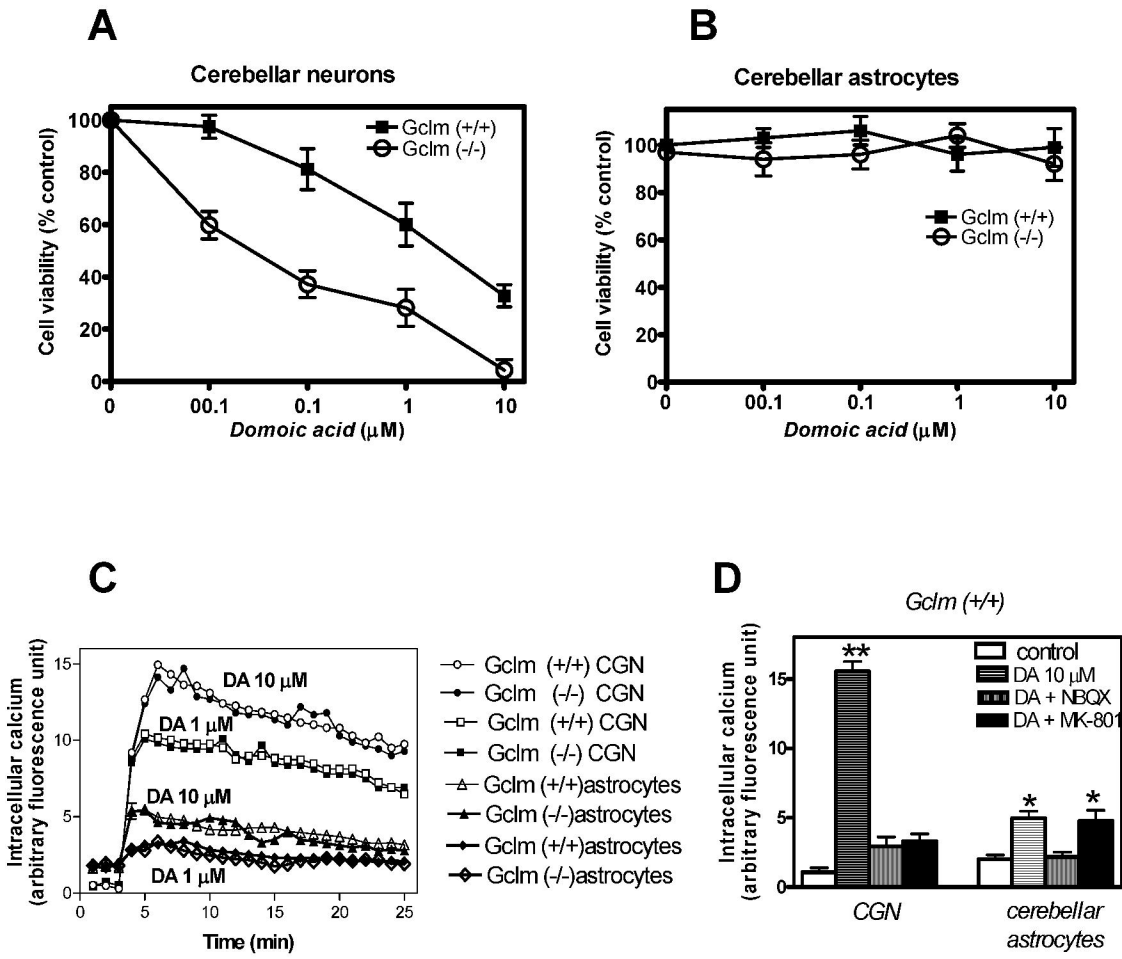
FIGURE 3
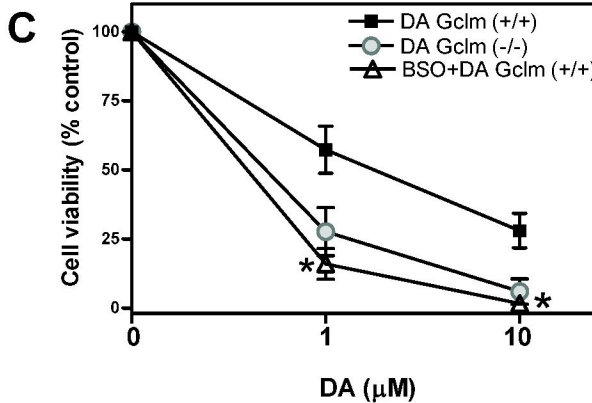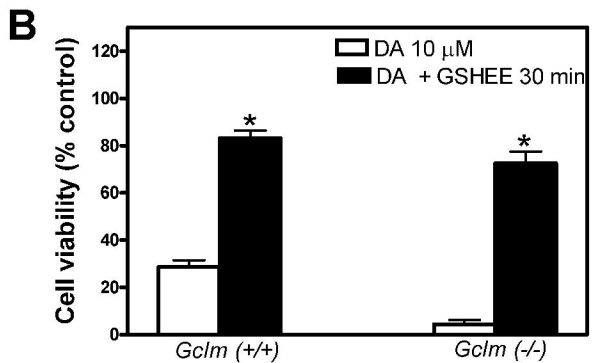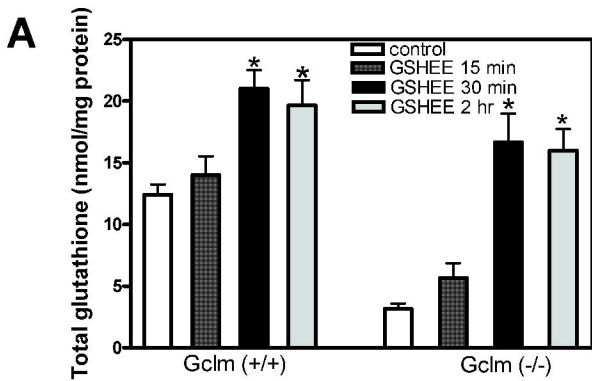
FIGURE 4
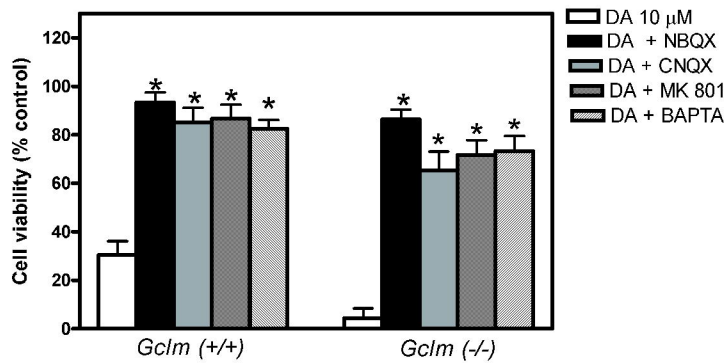
FIGURE 5

FIGURE 6

FIGURE 7

FIGURE 8

FIGURE 9